

Polyglycerol-Based Mucus-Inspired Hydrogels

Antara Sharma, Boonya Thongrom, Sumati Bhatia, Benjamin von Lospichl, Annalisa Addante, Simon Y. Graeber, Daniel Lauster, Marcus A. Mall, Michael Gradzielski,* and Rainer Haag*

The mucus layer is a hydrogel network that covers mucosal surfaces of the human body. Mucus has important protective properties that are related to its unique rheological properties, which are based on mucins being the main glycoprotein constituents. Mucin macromolecules entangle with one another and form a physical network that is instrumental for many important defense functions. Mucus derived from various human or animal sources is poorly defined and thus not suitable for many application purposes. Herein, a synthetic route is fabricated to afford a library of compositionally defined mucus-inspired hydrogels (MIHs). MIHs are synthesized by thiol oxidation to render disulfide bonds between the crosslinker ethoxylated trimethylolpropane tri(3-mercaptopropionate) (THIOCIURE ETTMP 1300) and the linear precursors, dithiolated linear polyglycerol (LPG(SH)₂) or polyethylene glycol (PEG(SH)₂) of different molecular weights. The mixing ratio of linear polymers versus crosslinker and the length of the linear polymer are varied, thus delivering a library of compositionally defined mucin-inspired constructs. Their viscoelastic properties are determined by frequency sweeps at 25 and 37 °C and compared to the corresponding behavior of native human mucus. Here, MIHs composed of a 10:1 ratio of LPG(SH)₂ and ETTMP 1300 are proved to be the best comparable to human airway mucus rheology.

gastrointestinal, reproductive, and oculo-rhino-otolaryngeal tract surfaces. It is involved in a diverse range of functions as a result of its unique properties. It prevents dehydration of the mucosa by maintaining a hydrated layer on the epithelial surface,^[1] and exhibits shear-thinning rheological behavior that supports its lubricant role by warranting a smooth passage for passing objects.^[2] In the respiratory tract, mucus entraps inhaled pathogens, allergens, and irritants that are constantly removed by mucociliary clearance driven by ciliary beating on airway surfaces facilitating constant mucus clearance from the lungs.^[3] Furthermore, the mucus layer serves as the external defense system of the body against pathogen attack in mucosal immunology.^[1,4,5] The mucus coating is a complex heterogenous biopolymer matrix comprising water (up to 97% by weight), mucin (typically about 5% by weight or less), inorganic salts (≈1% by weight), carbohydrates, proteins, antimicrobial peptides, and lipids. The physical behavior and resultant protective functions

of mucus are attributed to its constituents, particularly mucin glycoproteins,^[6] which represent more than 80% of the overall organic composition.^[7] Mucin macromolecules contain regions of high glycosylation. The sulfate ester and sialic acid motifs

1. Introduction

Mucus is a complex, viscoelastic hydrogel that protects the mucosal surfaces of the mammalian body, such as the respiratory,

A. Sharma, B. Thongrom, S. Bhatia, R. Haag
 Institut für Chemie und Biochemie
 Freie Universität Berlin, Takustraße 3, Berlin 14195, Germany
 E-mail: haag@chemie.fu-berlin.de


B. von Lospichl, M. Gradzielski
 Institut für Chemie
 Technische Universität Berlin
 Straße des 17. Juni 124, Berlin 10623, Germany
 E-mail: Michael.gradzielski@tu-berlin.de

A. Addante, S. Y. Graeber, M. A. Mall
 Department of Pediatric Respiratory Medicine, Immunology and Critical Care Medicine
 corporate member of Freie Universität Berlin and Humboldt Universität zu Berlin
 Charité – Universitätsmedizin Berlin
 Berlin 13353, Germany

A. Addante, S. Y. Graeber, M. A. Mall
 Berlin Institute of Health at Charité – Universitätsmedizin Berlin
 Berlin 10178, Germany

A. Addante, S. Y. Graeber, M. A. Mall
 associated partner site
 Deutsches Zentrum für Lungenforschung e. V.
 Aulweg 130, Gießen 35392, Germany

D. Lauster
 Institut für Chemie und Biochemie
 Fachbereich Biologie, Chemie, Pharmazie
 Freie Universität Berlin
 Arnimallee 22, Berlin 14195, Germany

 The ORCID identification number(s) for the author(s) of this article can be found under <https://doi.org/10.1002/marc.202100303>

© 2021 The Authors. Macromolecular Rapid Communications published by Wiley-VCH GmbH. This is an open access article under the terms of the Creative Commons Attribution-NonCommercial License, which permits use, distribution and reproduction in any medium, provided the original work is properly cited and is not used for commercial purposes.

DOI: 10.1002/marc.202100303

decorate the glycosyl end groups, which in turn act as decoys for various virus families. In addition, the network structure of mucus has an equally important role in mucosal immunology.^[8] The long, fibrillar structure of the mucin molecules enables intermolecular entanglement as well as various covalent and electrostatic interactions to form a gel matrix. The network structure provides multiple obstructions in the path of an incoming pathogen and prevents it from reaching the epithelial cell surface by essentially affecting its motility.^[8,9]

The invasion by pathogens to initiate the infection process is typically initiated by a compromised mucus barrier and thus the subsequent proliferation of infection. Respiratory viruses, such as the influenza A virus and SARS-CoV2 must pass through the mucus barrier to access the underlying epithelia and initiate the viral life cycle.^[2,4,10]

However, naturally occurring mucus is ineffectual for antiviral purposes due to its poorly defined composition, the challenges of extracting of sufficient amounts, the arduous purification required, and performance deviation as a result of a source-dependent composition.^[11] The use of synthetic mucus offers a controlled pathway to overcome such challenges and can, therefore, help to understand the role of different mucus compositions and functional properties in health and disease. The molecular structure, polymer length, and viscoelastic behavior can be precisely controlled while offering a reduction in heterogeneity typical to natural mucus.

Synthetic platforms for surface-tethered mucins have been designed and studied by Kramer et al.^[12] An analog of the peptide backbone of a mucin molecule bearing the *N*-GalNAc branching points native to mucus was constructed using *N*-carboxyanhydride polymerization. However, this model is designed specifically for transmembrane mucin modeling rather than application purposes. Mahalingam et al. devised an elegant platform for the fabrication of a mucus gel network, wherein the boronate-diol condensation reaction was employed to induce a stimuli-responsive network against HIV infection.^[13] This gel mimics cervicovaginal mucus, rather than presenting a broader mucus-mimetic approach. Other synthetic formulations have been explored which exploit the adhesive and lubricating properties of the gel.^[14] With the multivalent presentation of hydroxyl groups on MIHs, as well as the usage of a disulfide linkage, the gels will be even more customizable and closer to natural mucus.

The aim of the present work was to synthetically fabricate linear polyglycerol (LPG) and polyethylene glycol (PEG)-based gel systems that mimic certain characteristics of gel-forming mucus, with the goal of attaining rheological characteristics approaching those of naturally occurring gel-forming mucus of healthy human sputum.

In order to synthetically combine these properties, a highly water soluble, biocompatible, multivalent, and linear core scaffold was provided by thiolated linear polyglycerol^[14–16] (LPG(SH)₂). The multivalent backbone provided ample opportunity for creating a burgeoning synthetic glycosyl domain, akin to mucin. These molecules may be functionalized as required, thereby facilitating a certain influence on the rigidity. Mucus-inspired hydrogels (MIHs) were then realized by reacting these molecules with ethoxylated trimethylolpropane tri(3-mercaptopropionate)

ETTMP 1300 crosslinkers by thiol oxidation to form disulfide bonds, whereby their rheological properties were measured (**Figure 1**). Thus, by an amalgamation of facile techniques, a library of rheologically diverse, compositionally defined mucin-inspired hydrogels was developed. This model not only approaches the structural properties of natural mucus but also attains some of its primary functions without the hassle of lengthy and difficult reactions.

2. Results and Discussion

2.1. Design and Synthesis of Building Blocks

The network structure in natural mucus arises due to the physical and chemical properties imparted by mucin glycoproteins. There are cysteine end groups on every mucin glycoprotein that allow the long, fibrillar molecules to elongate further, resulting in the formation of a mucin “chain.”^[1,7] This results in the physical entanglement of the chains and a network structure arises. The crosslinking is further secured as the chains also interact with one another by hydrophobic and electrostatic means.^[2,15]

In order to develop components for MIHs, an ideal model would be one which allows easy modulation along the lines of viscoelasticity and pore size, while offering multiple backbone functionalization groups to enable multivalent sugar modifications. A chemically crosslinked hydrogel requires a linear structure interspersed with crosslinking points, in ratios that enable a target flexibility. A linear precursor in the MIH network would correspond to the mucin glycoprotein structure in naturally occurring gel mucus, exhibiting structural and functional similarity to it. It would incorporate reactive end groups to enable chain elongation and reaction with crosslinking agents.

The nature of crosslinking in naturally occurring gel mucus is relevant in determining the rheological properties of the network. Individual mucin molecules are linked to each other by disulfide bonds.^[7] Thus, such a reversible, redox-responsive bond should be present in the MIH system. Furthermore, the components should be able to react with each other under mild conditions at room temperature.

With these tools, a library of MIHs has been created with rheological properties, network mesh sizes, and backbone structures that approach the corresponding traits of naturally occurring mucus. Homobifunctionalized linear polyglycerol chains with thiol groups at both ends, i.e., LPG(SH)₂, were prepared as analogs of mucin glycoproteins in MIH networks. Moreover, the LPG backbone structures display multiple hydroxyl groups that equip these models for functionalization with various sugars or other functional groups found in mucin to enable future modification when necessary. The structural properties of MIHs can be regulated by altering the length of the LPG backbone or by replacing it with another linear structure altogether, thus facilitating rheological comparisons on the basis of backbone structure and rigidity. For this purpose, an LPG(SH)₂ backbone of molecular weight 5 kDa was designed (**Scheme 1**). For comparison, two more MIH families were synthesized with linear dithiofunctionalized polyethylene glycol PEG(SH)₂ of molecular weights 3 and 6 kDa (**Scheme 2**).

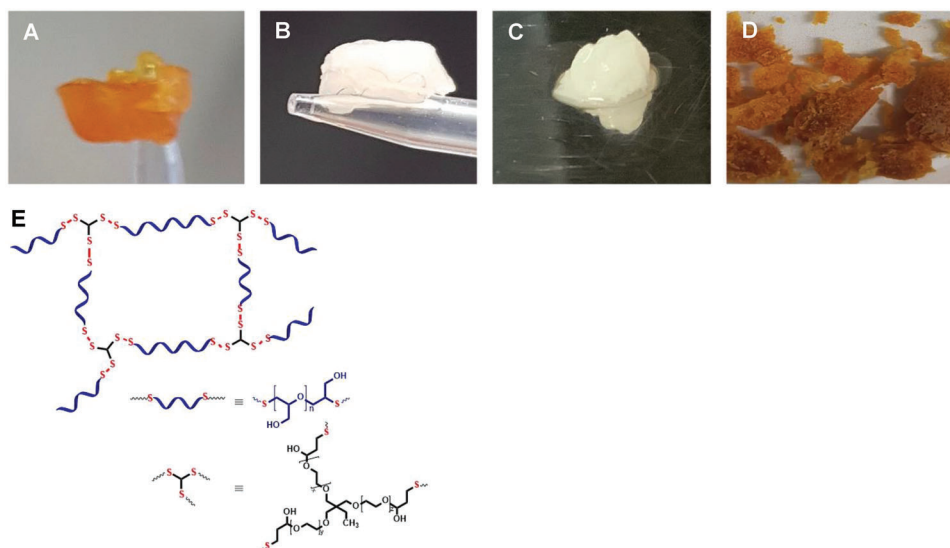
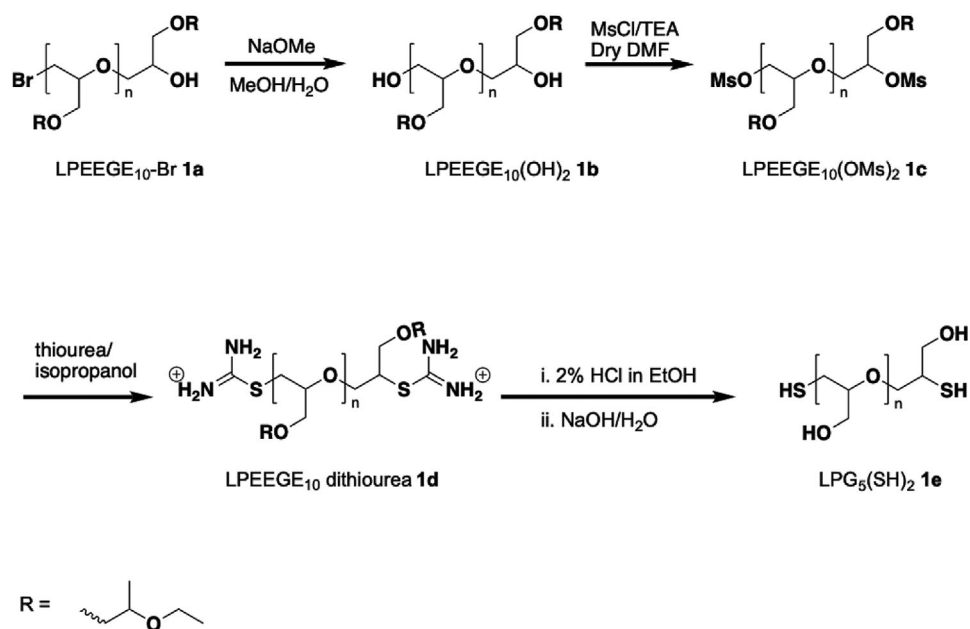
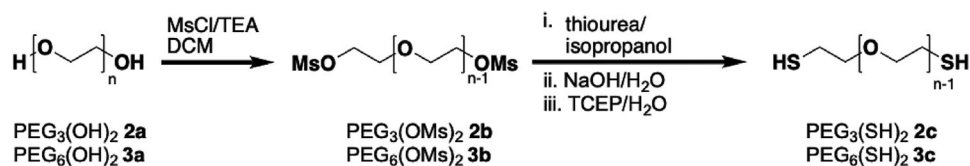


Figure 1. A) MIH-1a containing iodine traces; B) after iodine removal by PBS washing; C) the decrease in elasticity of MIH-1b with increasing linear component becomes visible by eye; D) the hard, coarse, and brittle solid formed upon oxidation of pure ETTMP; E) (right) scheme representing the network structure of MIHs composed of ETTMP 1300 and LPG(SH)₂; chemical structures of ETTMP 1300 (left) and LPG(SH)₂ (below).



Scheme 1. Synthesis of LPG(SH)₂ 1e.



Scheme 2. Synthesis of PEG(SH)₂ (2c and 3c).

2.1.1. Synthesis of Dithiolated LPG(SH)₂ 1e

The bromine-capped linear polyethoxyethyl glycidyl ether (LPEEGE-Br) was synthesized by anionic ring-opening polymerization following the procedure reported in the literature.^[16] LPG(SH)₂ was synthesized in three steps. LPEEGE-Br with molecular weight 10 kDa **1a** was hydrolyzed under basic conditions (pH > 10), resulting in the formation of linear polyethoxyethyl glycidyl ether (LPEEGE-(OH)₂ **1b** with two terminal hydroxy groups. This was followed by a mesylation reaction. The mesylated product **1c** was reacted with thiourea to obtain LPEEGE dithiourea **1d** as the substitution product. The nitrogen and sulfur contents were estimated by elemental analysis to corroborate the degree of conversion. The final compound LPG₅(SH)₂ **1e** was obtained after acidic and basic hydrolysis of ethoxyethyl and thiourea groups, respectively (Scheme 1). Tris(2-carboxyethyl)phosphine (TCEP) was added to this mixture as a reducing agent. Subsequent dialysis led to pure products. ¹H NMR analysis at each step corroborated the formation and purity of the compound. The presence of 2 thiol groups per chain was confirmed by elemental analysis and ¹H NMR studies.

2.1.2. Synthesis of PEG(SH)₂ 2c and 3c

Dithiolated PEGs with molecular weights 3 kDa PEG₃(SH)₂ and 6 kDa PEG₆(SH)₂ were synthesized following an approach modified from the original report from Mahadevegowda and Stuparu (Scheme 2).^[17] First homo-bifunctional dihydroxy PEGs, i.e., PEG₃(OH)₂ **2a** and PEG₆(OH)₂ **3a** were mesylated under anhydrous conditions. PEG₃(OMs)₂ **2b** and PEG₆(OMs)₂ **3b** were obtained as a white powder upon precipitation of the reaction mixture. Thiolation of the thus obtained PEG(OMs)₂ was then performed with thiourea under elevated temperature, followed by basic hydrolysis and reduction by TCEP to finally yield PEG₃(SH)₂ **2c** and PEG₆(SH)₂ **3c** as pale yellow powder after precipitation.

2.2. Synthesis of Mucus-Inspired Hydrogels (MIHs)

In order to assess whether hydrophilic linear polyglycerols can provide mucus-like hydrogels with matching rheological characteristics, a commercial homotrifunctionalized PEG thiol, ETTMP 1300 was used as the crosslinker. Gelation was induced by simply oxidizing the thiol groups present on both of the macromonomer components in the presence of hydrogen peroxide and NaI solution in water.^[18] A 3D matrix was consequently formed with thiol-disulfide interchange reactions facilitating certain characteristic rheological properties of such networks.

Several MIH families were synthesized and compared on the basis of their structure as well as the molecular weight of the linear scaffold. Thus, three gel families were assembled using LPG(SH)₂ and PEG(SH)₂ of varying lengths as linear precursors: LPG₅(SH)₂ **1e**, PEG₃(SH)₂ **2c**, and PEG₆(SH)₂ **3c**. Furthermore, the ratio of the crosslinker to the mucin analog component was varied while maintaining a constant gel volume of every gel family, allowing the rheological properties to be fine-tuned.

In Table 1, all the studied gels are listed with their corresponding synthetic details. Thiol oxidation is a sensitive procedure,

Table 1. Description of various MIH gel series studied. The gels are classified by series depending upon the linear precursors of which they are composed. Different types of MIHs within each series are fabricated by changing the ratios of ETTMP 1300 crosslinker to the linear component, thus rendering a total of 12 gels. A total gel volume of 200 μL was fixed for every composition.

MIH series	Linear precursor	Ratio of ETTMP 1300 crosslinker to linear component			
		1:3	1:7	1:10	1:14
MIH-1	LPG ₅ (SH) ₂	MIH-1a	MIH-1b	MIH-1c	MIH-1d
MIH-2	PEG ₃ (SH) ₂	MIH-2a	MIH-2b	MIH-2c	MIH-2d
MIH-3	PEG ₆ (SH) ₂	MIH-3a	MIH-3b	MIH-3c	MIH-3d

with the possibility of oxidation side products such as sulfenic, sulfinic, and sulfonic acids.^[19] These side products may have inhibitory effects on gel formation. To circumvent this problem, the amount of oxidizing agent needs to be slightly decreased with increasing linear component amounts in order to account for the disparity in the overall thiol content.

The gelation process could be visually monitored as the color of the pre-gel mixture deepened from a cloudy white solution to an orange-brown semi-solid upon oxidation. The gels were kept for some time so that an equilibrium state could be attained. Thereafter rheology studies were conducted. The color transition indicates formation of I₂ (Figure 1A). In order to remove the iodine side product from the gels, all MIHs were incubated for 24 h in phosphate-buffered saline (PBS) solution. A change of color thus followed, from the iodide-characteristic orange color to an opaque, white gel, which otherwise retained all other properties (Figure 1B).

2.3. Rheology

2.3.1. Oscillatory Rheology

The mechanical properties of a gel can be defined by its viscoelastic properties, which in turn can be determined by oscillatory rheology measurements. A study of the viscoelastic properties of the LPG- and PEG-based scaffolds was done with the aim to establish relationships between the viscoelastic properties of MIHs and their respective constitution. The results thus obtained were compared with corresponding values in naturally occurring mucus to identify systems with similar rheological properties.

The specifications of the LPG-based MIH-1 gels, and PEG-based MIH-2 and MIH-3 gels studied are listed in Table 1. The gels compared were based on three scaffolds—LPG₅(SH)₂, PEG₃(SH)₂, and PEG₆(SH)₂. The ratio of the linear precursor to the crosslinking component, ETTMP 1300, was varied in each case. The concentration of the crosslinker was decreased steadily while maintaining a constant amount of polymer dithiols used overall. This then should lead to increasingly less crosslinked hydrogel networks.

The rheological properties of all the hydrogels were characterized in terms of the storage *G'* and loss *G''* moduli obtained from oscillatory shear experiments. First, a strain-sweep test was conducted to determine the linear viscoelastic region (LVE).

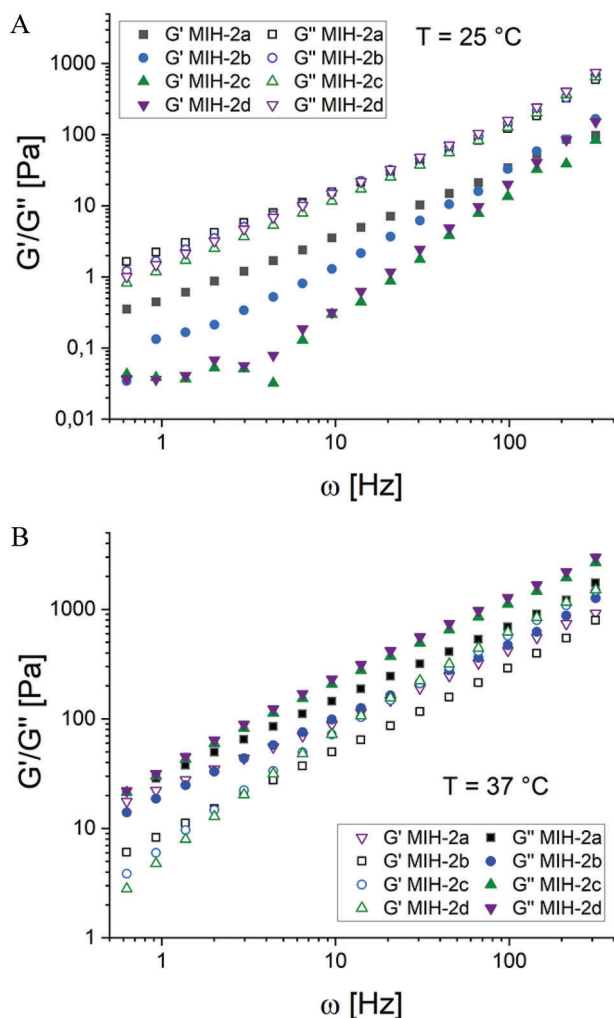


Figure 2. Storage (G') and loss (G'') modulus as function of the radial frequency ω of MIH-2 A) at 25 °C; B) at 37 °C, for samples where the crosslinker density was varied systematically.

Then oscillatory rheology experiments, specifically oscillatory shear and strain tests, were conducted in the LVE to determine G' and G'' as functions of radial frequency ω . The oscillatory rheology results for hydrogels with $\text{PEG}_3(\text{SH})_2$ and $\text{PEG}_6(\text{SH})_2$ are shown in **Figures 2** and **3**, respectively; data for gels with $\text{LPG}_5(\text{SH})_2$ are shown in **Figure 4**. Each test was conducted at 25 °C and at the physiological temperature of 37 °C.

For the PEG-based compounds (MIH-2 and MIH-3), a rather linear increase of G' and G'' can be seen in a double-logarithmic plot, where for the longer PEG spacer (MIH-3) G'' is typically higher than G' , which indicates that these systems are dominated by their viscous properties. This also indicates that these systems are not really proper gels, but at best can be classified as soft and gel-like, i.e., a viscoelastic fluid. They are not permanently crosslinked and are relaxing under a given stress proportional to the time left for this relaxation. Interestingly, with increasing temperature both moduli increase substantially (by more than a factor 10) and the increase is larger for G' , i.e., the relative elastic properties of these gels increase with rising temperature. As

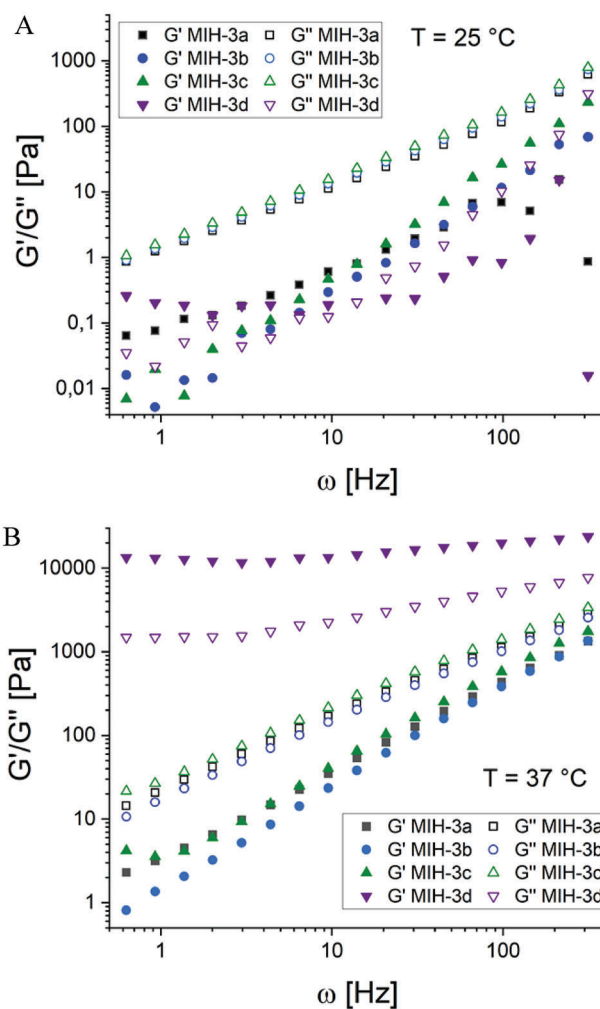


Figure 3. Storage (G') and loss (G'') modulus as function of the radial frequency ω of MIH-3 A) at 25 °C; B) at 37 °C, for samples where the crosslinker density was varied systematically.

stated before, this behavior may be attributed to the fact that PEG becomes less well soluble in water with increasing temperature and therefore the network structure would be contracting. This slope of the frequency increase was higher for G' ($\approx \omega^{1.2}$, at 37 °C) than for G'' ($\approx \omega^{0.85}$, at 37 °C) and accordingly with increasing frequency the gap between G'' and G' decreases. This suggests that the crossover point where G' would overtake G'' would take place at frequencies higher than the frequency range applied here, indicating a rather short structural relaxation time of less than 0.02 s.

Generically similar is the behavior of the PEG-based systems with the shorter PEG spacer (MIH-2), but here the relative increase of G' with rising temperature is even much more marked. Upon going from 25 to 37 °C, it increases by a factor of 30–200, while G'' only increases by a factor of 3–5. This also means that at low temperature the systems are dominated by viscous properties, but this is reversed at 37 °C, where the elastic properties become dominant. Interestingly, the scaling of both G' and G'' at 37 °C is about $\approx \omega^{0.75-0.8}$.

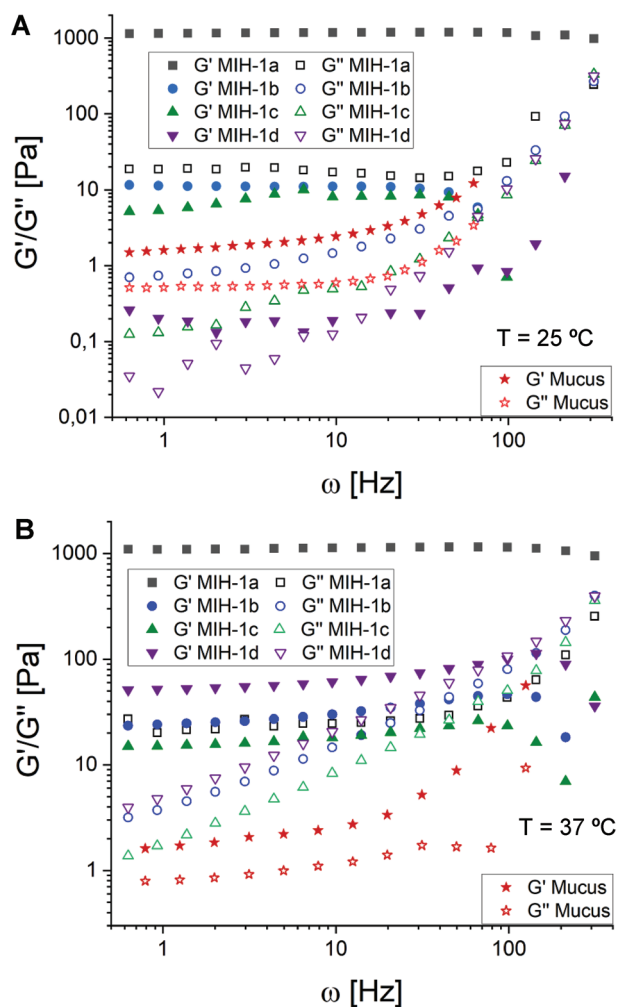


Figure 4. Storage modulus G' and loss modulus G'' as functions of the radial frequency ω of A) MIH-1 at 25 °C; B) MIH-1 at 37 °C, for samples where the crosslinker density was varied systematically. For comparison, data of fresh airway mucus obtained from healthy donors were also included in (A) (averaging over three different samples).

In contrast, for $\text{LPG}_5(\text{SH})_2$ -based MIH-1 gels, both moduli, G' and G'' , remained rather constant, with G' being much larger than G'' , i.e., they behaved like typical gels with a yield stress. For instance, for the sample with thrice the linear component as compared to the crosslinker (MIH-1a), G' remained about two orders of magnitude higher than G'' throughout the frequency range, thus showing gel-like behavior. For the other gels with less crosslinker, G' remained also constant, but at much lower frequency values. Compared to the PEG-based gels the increase of viscoelastic parameters is much less pronounced here.

Even more different is the behavior of G'' that increases markedly with rising frequency in the higher frequency range and there even bypassing G' , although also G' starts to increase somewhat for frequencies above 10 Hz. Such behavior is not very frequently seen, but has for instance similarly been reported for carrot puree.^[20] Generally, it indicates a faster relaxation process being present within the system.

Table 2. Shear modulus G_0 and estimated mesh size ξ of $\text{LPG}_5(\text{SH})_2$ -based MIHs at 25 and 37 °C.

MIH	[crosslinker]/[linear component]	25 °C		37 °C	
		Shear modulus [G_0 /Pa]	Mesh size [ξ /nm]	Shear modulus [G_0 /Pa]	Mesh size [ξ /nm]
MIH-1a	1:3	1157	15	1112	15
MIH-1b	1:7	11	72	33	52
MIH-1c	1:10	8	82	19	61
MIH-1d	1:14	0.2	286	69	40

A direct comparison of the rheological properties of healthy human airway mucus with MIHs can be very interesting in this context. Previous experiments have shown that the shear modulus of mucus in healthy lungs is ideally around 1–2 Pa.^[21] To compare synthesized MIHs with human mucus, rheological properties of healthy airway mucus from three individual donors were determined and are included in Figure 4. It can be seen that human mucus also shows such an upturn above 10 Hz in a similar fashion for G' and G'' , while at lower frequency a constant plateau is observed, with $G' \sim 2$ Pa. It is interesting to note that the rheological properties of mucus are rather insensitive to the temperature change from 25 to 37 °C (while the synthetic gels generally show some increase especially of the storage modulus, which can be attributed to the effect of entropy elasticity for covalently bound networks). Comparing the data in Figure 4, one can conclude that MIH-1 with a ratio of crosslinker to linear component in the range of 1:10 to 1:14 is showing rather similar rheological behavior as healthy airway mucus. Thus, the rheological data show that tunable hydrogels can be constructed, where storage and loss moduli, and to some extent even their frequency dependence, can be controlled via the ratio of the linear component to the crosslinking agent.

The marked decrease of the elastic properties with decreasing content of crosslinker could be attributed to a decreasing number of crosslinking points within the gel network, but given the large decrease it would not just mean less crosslinker but also a substantially reduced crosslinking efficiency. In order to quantify this further, we determined the shear modulus G_0 as the average of G' in the plateau regime and the corresponding values are given in Table 2. Especially at lower crosslinker content, an increase in temperature had a similar but smaller effect on the LPG-based MIHs as observed for the PEG-based MIHs, i.e., the elastic properties increase at the higher temperature. An explanation for that behavior would be that the linking polymer chains are less well dissolved in water with increasing temperature and therefore they swell less and correspondingly their crosslinking density increases. The effective network mesh sizes ξ were then estimated from the shear modulus G_0 from the simplified relation: $G_0 = kT/\xi^3$ and they are given in Table 2.^[22]

The mesh size ξ of a network (which is the inverse of the crosslinking density) is directly linked to its rheological properties. The rough estimate obtained from the shear modulus G_0 (Table 2, Figure 5) yields ξ values in the range of 15–80 nm, which compares well with the experimentally observed values of

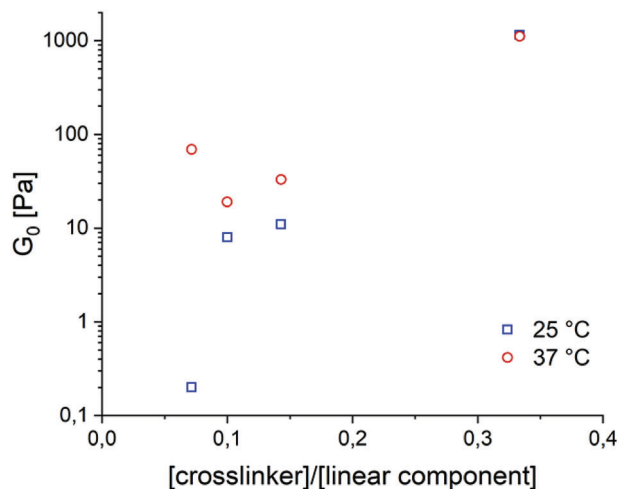


Figure 5. Shear modulus G_0 for the MIH-1 gels as a function of the ratio of crosslinker to linear component, measured at 25 and 37 °C.

Table 3. Crosslinking densities obtained by Equation (1).

MIH type	25 °C $\mu\text{mol cm}^{-3}$	37 °C $\mu\text{mol cm}^{-3}$
MIH 1a	0.44	0.45
MIH 1b	0.0099	0.0043
MIH 1c	0.0062	0.0023
MIH 1d	0.021	0.000072

20–200 nm for naturally occurring mucus.^[23] While the data differ depending upon the source and method of examination, a mesh size in the range of 100 nm up to even a few micrometers is the norm.^[24] This observation also aligns with the inferred rheological data. As shown in Table 2, for MIH-1c the effective mesh sizes at physiological temperature were about 60 nm and thus in the same range as the desired size range. With the tunable design of such systems, much larger pore sizes can be achieved by substitution of backbone structures or crosslinkers of different lengths.

The effective crosslinking density ρ can be estimated from the rheological data via Equation (1):

$$\rho = \frac{G'_{\text{plateau}}}{R \cdot T} \quad (1)$$

This equation is based on the plateau modulus G'_{plateau} obtained during frequency sweep experiments, where R is the universal gas constant, and T is the temperature. The effective rheological crosslinking density is simply the inverse of the mesh size given in Table 2, and listed in Table 3.

The observed effective crosslinking density decreases substantially with lowering the content of the crosslinker. For comparison one can also calculate the crosslinking density, as it would be expected for perfect polymerization, and for this assumption one obtains values within the limits of 2 – 20 $\mu\text{mol cm}^{-3}$, depending on the gel composition. This indicates that the chemical crosslinking is only effective to a rather low extent and correspondingly one has a much more open structure than would be

present for complete crosslinking. In addition, one has to note that Equation (1) is just a general relation and depending on the precise topology of the network one would have a prefactor different than one, which to a lesser extent may also attribute to the observed discrepancy of values.

3. Conclusion

In this work, the endeavor was to create such a mucus-inspired hydrogel in a facile, low-cost manner with a nature-inspired disulfide crosslinking chemistry. For this purpose, LPG and PEG chains of different molecular weights were utilized to produce dithiol-functionalized chains, which in turn were gelled with ETTMP 1300—a tri-PEG crosslinker, in the presence of an oxidizing agent. Of the formed gels, the most appropriate for the intended purpose was the MIH-1c gel based on a LPG-dithiol with an Mn of 5 kDa. At lower frequencies, the gel showed elastic-dominant behavior, with G' falling in the range of 5–10 Pa at 25 °C. As for all other gels, the G' increased to 15–20 Pa in the same frequency range as the temperature was increased to 37 °C. Thus, we successfully demonstrated the synthesis of mucus-like hydrogels with a range of rheological properties and achieved with MIH-1c a hydrogel that has rheological properties comparable to native human airway mucus.

4. Experimental Section

Materials: All chemicals were obtained from Merck (Darmstadt, Germany) and Acros Organics (Geel, Belgium), and used without any purification. ETTMP 1300 was received as a gift from Bruno Bock (Marschacht, Germany) and used as such. Moisture-sensitive reactions were performed under anhydrous conditions, in flame-dried glassware. Reflux reactions were performed at 115 °C in an oil bath. Dialysis was performed in Spectra Por dialysis tubing (MWCO = 2000 g mol⁻¹) (Carl Roth GmbH, Karlsruhe, Germany). The dialysate was changed five times within 2 days. ¹H NMR spectra were recorded in AV 500 spectrometer (Bruker, Massachusetts, USA). NMR chemical shifts were reported as δ values in ppm. LPEEGE with average molecular weights of 10 kDa (LPEEGE₁₀) were synthesized by following procedures reported in literature.^[15]

Methods: Synthesis and Characterization of Dithiolated Linear Polyglycerol LPG(SH)₂: **Synthesis of LPEEGE 1a:** LPEEGE-Br was synthesized as described previously.^[16] LPEEGE₁₀Br **1a** (2 g, 2.38 × 10⁻² mmol) was dissolved in a mixture of MeOH (18 mL) and H₂O (3 mL). Sodium methoxide (30 wt%, 200 μL , 0.88 mmol) was added to the solution and stirred overnight at room temperature. The crude LPEEGE product was then purified by dialysis against acetone (2 days) to remove excess sodium methoxide as well as to remove methanol and water to afford pure LPEEGE₁₀(OH)₂ **1b** (1.9 g, 95% yield).

Synthesis of LPEEGE₁₀ dithiourea 1d: Thoroughly dried LPEEGE₁₀(OH)₂ **1b** (1.9 g, 2.4 × 10⁻² mmol, 1 eq.) was dissolved in anhydrous dimethylformamide (DMF, 250 mL), followed by the addition of triethylamine (TEA, 25 μL , 1.3 mmol, 7.5 equivalent) to the stirring solution. The reaction flask was cooled over an ice bath, and subsequently a solution of MsCl (5.5 μL , 7.14 × 10⁻² mmol, 3 eq.) in DMF (1.5 mL) was added in a dropwise manner to the vigorously stirring solution. The reaction mixture was stirred over an ice bath for 1 h, after which the solution was allowed to attain room temperature and continued to be stirred for 48 h. After solvent removal, the crude product was dialyzed against a 3:1 chloroform–methanol mixture for 24 h. The resultant yellow-orange-colored LPEEGE₁₀(OMs)₂ (**1c**) had a honey-like consistency (yield: 50%) which was used for the dithiourea formation without any delay.

In order to afford thiol-functionalized LPEEGE₁₀(SH)₂, LPEEGE₁₀(OMs)₂ **1c** (1.9 g, 2.4 × 10⁻² mmol) was dried under vacuum, and then dissolved in mixture of 1-propanol (200 mL) and MeOH

(10 mL). The reaction was refluxed for 48 h after thiourea (73 mg, 9.52 × 10⁻¹ mmol, 4 eq.) was added. 1-propanol was evaporated to afford crude LPEEGE₁₀ dithiourea **1d**, which was then purified by dialysis using methanol as a solvent. Its constitution was confirmed by elemental analysis; N = 0.716; C = 46.66; S = 0.297; H = 7.578 (≈2 thiol groups per chain). LPEEGE₁₀ dithiourea **1d**, 95% isolated yield, ¹H NMR (500 MHz, MeOD, δ (ppm)): 1.17–1.30 (m, 11H), 3.88–4.11 (m, LPG backbone), 7.91 (s, 4H).

Synthesis of LPG₅(SH)₂ 1e: An acidic solution of ethanol was prepared by mixing HCl in ethanol such that the solution had a pH of 5. LPEEGE₁₀ dithiourea **1d** was dissolved in 150 mL of the prepared acidic solution and then stirred overnight, after which the pH of the solution was brought up to 8 using 1 M NaOH solution. Sodium hydroxide (4 mg, 0.1 mmol, 4 eq.) was added to an aqueous solution of the crude product, which was then refluxed for 48 h. The temperature of the reaction flask was brought down to room temperature. After the reaction, crude product was dialyzed against deionized water for 72 h to finally obtain pure LPG(SH)₂ **1e** in ≈95% isolated yield which was stored in the presence of TCEP.

Synthesis and Characterization: Dithiolated PEG (PEG₃(SH)₂): **Synthesis of Dimesylated PEG (PEG(OMs)₂):** Dry PEG₆(OH)₂ **3a** (20 g, 3.3 mmol, 1 eq.) was dissolved in anhydrous dichloromethane (DCM, 100 mL). TEA (2.77 mL, 20 mmol, 6 equiv.) was injected in this solution. The reaction flask was then cooled over ice bath followed by subsequent dropwise addition of methane sulfonyl chloride (1.03 mL, 13.3 mmol, 4 equiv.). The reaction was allowed to run for 1 day. Afterward the crude product was purified by first washing the reaction mixture thrice with brine, drying the DCM layer, and then precipitating the resultant product in cooled diethylether. The precipitate so obtained was collected and dried in vacuo over 24 h to obtain PEG(OMs)₂ as a white colored powder.

PEG₃(OMs)₂ **2b**: 90% isolated yield, ¹H NMR (700 MHz, CDCl₃, δ (ppm)): 3.07 (3H, s), 3.63–3.76 (m), 4.36 (2H, t, J = 7 Hz)

PEG₆(OMs)₂ **3b**: 95% isolated yield, ¹H NMR (500 MHz, CDCl₃, δ (ppm)): 3.07 (3H, s), 3.48–3.78 (m), 4.37 (2H, t, J = 5 Hz)

Synthesis of Dithiolated PEG (PEG(SH)₂): To a solution of dimesylated PEG (PEG₆(OMs)₂ **3b** (19 g, 3.2 mmol, 1 eq.) in 1-propanol (100 mL), thiourea (1.02 g, 13.3 mmol, 4 eq.) was added and the solution was refluxed for 24 h to obtain diisothiuronium PEGintermediate. 1-propanol was then removed from the crude mixture and NaOH (0.53 g, 13.3 mmol, 4 eq.) and water (100 mL) were added. This solution was then refluxed for 24 h. Afterward, the crude mixture was neutralized to pH 7. TCEP (1.67 g, 6.7 mmol, 2 eq.) was consequently added, and the reaction was stirred for a further 2 h to obtain the crude final PEG-dithiol product. The product was purified following a precipitation procedure. To this end, NaCl was first added to the reaction mixture until the saturation point was attained. The product was then extracted with DCM. Thereafter, the DCM layer was dried with Na₂SO₄. Finally, the pure product was precipitated in cooled diethylether followed by drying in vacuo so as to obtain PEG(SH)₂ as a pale yellow colored powder.

PEG₃(SH)₂ **2c**: 79% isolated yield, ¹H NMR (600 MHz, CDCl₃, δ (ppm)): 1.59 (1H, t, J = 6 Hz, 12 Hz), 2.69 (2H, quat, J = 6 Hz, 12 Hz), 3.51–3.76 (m). Elemental analysis; N = 0.24; C = 53.43; S = 2.43; H = 8.52

PEG₆(SH)₂ **3c**: 88% isolated yield, ¹H NMR (500 MHz, CDCl₃, δ (ppm)): 1.59 (1H, t, J = 5 Hz, 10 Hz), 2.69 (2H, quat, J = 5 Hz, 10 Hz), 3.48–3.78 (m). Elemental analysis; N = 0.13; C = 54.24; S = 2.02; H = 8.47

Synthesis of MIHs: LPG-based and PEG-based gels were both fabricated in a manner that resulted in gels with the same volumes. Four families of gels were prepared, differing only by their linear components, namely, LPG₅(SH)₂, PEG₃(SH)₂, and PEG₆(SH)₂, listed as gel series **MIH-1**, **MIH-2**, and **MIH-3** in Table 2, respectively. Furthermore, the crosslinker to linear component ratios within each series was varied in order to zero in on the gels with the most promising rheological properties. Three such ratios for each series were inspected, and thus a total of 12 gel types were finally examined, the specifications of which are also listed in Table 2.

First, separate 50% w/v aqueous solution of the linear component was prepared in water. Similarly, a 50% w/v solution was also prepared for

ETTMP 1300. A 10 × 10⁻³ M NaI solution was freshly prepared. The two gel components were then mixed in an Eppendorf tube, in amounts as listed in Table 2, with the final crosslinker to backbone ratios being 1:3, 1:7, 1:10, and 1:14, respectively. NaI and H₂O₂ were added consecutively. This cloudy pregel solution was then vortexed until a color change from white to yellow was observed indicating the release of iodide and consequent formation of the tri-iodide ion. The color deepened within the next 2 min to finally develop into an orange-brown semi-solid. The gel was incubated at room temperature overnight in a closed container, and rheology tests were conducted thereafter.

The saturated yellow color of the gel was a leftover of the oxidation process, and easily be removed by incubation of the formed gel in PBS buffer for 24 h to obtain a white gel (Figure 1B). All gels were synthesized following the same gelation procedure.

Human Lung Sputum Samples: Collection of airway mucus samples from healthy donors was approved by the ethics committee of the Charité – Universitätsmedizin Berlin and written informed consent was obtained from all participants. All donors were healthy nonsmokers. Lung sputum was collected after induction by inhalation of hypertonic saline (NaCl 6%) with a PARI LC PLUS nebuliser (PARI GmbH, Starnberg, Germany) according to a standard operating procedure. Macrorheology was measured immediately using the Kinexus Pro + rheometer (NETZSCH GmbH, Selb, Germany) at 25 °C.

Rheological Analysis: The hydrogels were measured using a stress-controlled MCR 501 Anton Paar rheometer with a plate–plate stainless steel geometrical setup. A 25 mm upper rotating plate diameter was used for all measurements with constant gap size of 0.15 mm. The measurements were conducted at room temperature (25 °C) as well as physiological temperature (37 °C). The samples were allowed to reach temperature equilibrium for ≈5 min prior to each measurement.

Oscillatory Rheology: First, an amplitude sweep was performed to determine the limits of the LVE for each type of hydrogel analyzed in this study. The critical deformation strain was found to be at about 1%. The shear strain (γ) is defined as the ratio of the deflection path (s) to the shear gap (h)

$$\gamma = \frac{s}{h} \quad (2)$$

Next, oscillatory shear tests were conducted within the LVE region, applying a constant strain amplitude, γ_A, of 1%. Frequency sweeps of the hydrogel samples were conducted in the range 0.1–50 Hz. From the experimentally determined shear stress τ_A, storage modulus G' and loss modulus G'' were determined, which are related to each other via the phase angle (δ)

$$\tan \delta = \frac{G''}{G'} \quad (3)$$

The loss modulus G'' describes the viscous behavior of the sample which in turn is the result of energy dissipation due to the internal friction between the moving layers. Conversely, the storage modulus G' describes the energy stored elastically within the internal material structure as it is sheared.

Moreover, the rheological data could also be used to draw information on the internal hydrogel structure and to roughly estimate an effective mesh size, ξ, from the number density, ¹N, of crosslinking points, the Boltzmann constant k_B, absolute temperature T, and the plateau modulus G₀:

$${}^1N = \frac{G_0}{k_B T} = \frac{1}{\xi^3} \quad (4)$$

Hysteresis curves were produced for all frequency sweeps in order to ascertain the reproducibility of the data. All reported results were the average of the up- and down-ramps at each data point. The rheological properties of all three families of LPG- and PEG-based hydrogels were investigated on this basis.

Supporting Information

Supporting Information is available from the Wiley Online Library or from the author.

Acknowledgements

This study was supported by the Helmholtz Graduate School for Macromolecular Bioscience and funded by the Deutsche Forschungsgemeinschaft (DFG, German Research Foundation)—SFB 1449—projects A01, B03, C04, and Z02 and by the German Federal Ministry of Education and Research (82DZL0098B1). The rheometer employed was financed by the Deutsche Forschungsgemeinschaft (DFG, German Research Foundation) via grant GR1030/24-1. S.Y.G. is participant in the BIH-Charité Clinician Scientist Program funded by the Charité – Universitätsmedizin Berlin and the Berlin Institute of Health.

Open access funding enabled and organized by Projekt DEAL.

Conflict of Interest

The authors declare no conflict of interest.

Data Availability Statement

Research data are not shared.

Keywords

bio-inspired hydrogels, linear polyglycerol, mucus, redox responsive hydrogels

Received: May 12, 2021

Revised: July 23, 2021

Published online: September 13, 2021

- [1] R. Bansil, B. S. Turner, *Curr. Opin. Colloid Interface Sci.* **2006**, *11*, 164.
- [2] R. A. Cone, *Adv. Drug Delivery Rev.* **2009**, *61*, 75.
- [3] M. A. Mall, *J. Aerosol Med. Pulm. Drug Delivery* **2008**, *21*, 13.
- [4] D. J. Thornton, *Proc. Am. Thorac. Soc.* **2004**, *1*, 54.
- [5] M. R. Knowles, R. C. Boucher, *J. Clin. Invest.* **2002**, *109*, 571.
- [6] D. Song, D. Cahn, G. A. Duncan, *Langmuir* **2020**, *36*, 12773.
- [7] N. A. Peppas, Y. Huang, *Adv. Drug Delivery Rev.* **2004**, *56*, 1675.
- [8] M. Caldara, R. S. Friedlander, N. L. Kavanaugh, J. Aizenberg, K. R. Foster, K. Ribbeck, *Curr. Biol.* **2012**, *22*, 2325.
- [9] H. C. Berg, L. Turner, *Nature* **1979**, *278*, 349.
- [10] K. Ribbeck, *Biosci. Hypotheses* **2009**, *2*, 359.
- [11] C. Nowald, A. Penk, H.-Y. Chiu, T. Bein, D. Huster, O. Lieleg, *Macromol. Biosci.* **2016**, *16*, 567.
- [12] J. R. Kramer, B. Onoa, C. Bustamante, C. R. Bertozzi, *Proc. Natl. Acad. Sci. U. S. A.* **2015**, *112*, 12574.
- [13] A. Mahalingam, J. I. Jay, K. Langheinrich, S. Shukair, M. D. Mcraven, L. C. Rohan, B. C. Herold, T. J. Hope, P. F. Kiser, *Biomaterials* **2011**, *32*, 8343.
- [14] C. Werlang, G. Cárcarmo-Oyarce, K. Ribbeck, *Nat. Rev. Mater.* **2019**, *4*, 134.
- [15] X. Cao, R. Bansil, K. R. Bhaskar, B. S. Turner, J. T. Lamont, N. Niu, N. H. Afdhal, *Biophys. J.* **1999**, *76*, 1250.
- [16] M. Gervais, A. - L. Brocas, G. Cendejas, A. Deffieux, S. Carlotti, *Macromolecules* **2010**, *43*, 1778.
- [17] S. H. Mahadevegowda, M. C. Stuparu, *Eur. J. Org. Chem.* **2017**, *2017*, 570.
- [18] B. D. Fairbanks, S. P. Singh, C. N. Bowman, K. S. Anseth, *Macromolecules* **2011**, *44*, 2444.
- [19] J.-P. R. Chauvin, D. A. Pratt, *Angew. Chem., Int. Ed. Engl.* **2017**, *56*, 6255.
- [20] H. Moritaka, S.-I. Sawamura, M. Kobayashi, M. Kitade, K. Nagata, *Biosci., Biotechnol., Biochem.* **2012**, *76*, 429.
- [21] S. K. Lai, Y.-Y. Wang, D. Wirtz, J. Hanes, *Adv. Drug Delivery Rev.* **2009**, *61*, 86.
- [22] M. S. Green, A. V. Tobolsky, *J. Appl. Phys.* **1946**, *17*, 407.
- [23] H. M. Yildiz, C. A. Mckelvey, P. J. Marsac, R. L. Carrier, *J. Drug Targeting* **2015**, *23*, 768.
- [24] J. Leal, H. D. C. Smyth, D. Ghosh, *Int. J. Pharm.* **2017**, *532*, 555.